



GPS constraints on vertical crustal motion in the northern Basin and Range

Richard A. Bennett,¹ Sigrún Hreinsdóttir,¹ M. Soledad Velasco,¹ and Noah P. Fay¹

Received 30 July 2007; revised 26 September 2007; accepted 15 October 2007; published 30 November 2007.

[1] We estimated vertical velocities using an array of 12 continuous GPS stations forming part of the PBO NUCLEUS network. We analyzed data spanning the period 1996 through 2006. The array has an aperture ~ 400 km and crosses a major active intracontinental normal fault system in the northern Basin and Range province. The root-mean-square (RMS) of vertical rates relative to a local “no net vertical” frame is 0.3 mm/yr, indicating high relative rate precision. The RMS difference between rates based on $\Delta t \leq 7$ -year sub-strands of the total data set and the full ~ 10 -year rate estimates varies as $2.4 \Delta t^{-1.3}$ mm/yr. The net vertical rate observed across the greater Wasatch fault zone is consistent with the predictions of elastic half-space dislocation models only when the deep slipping part of the fault has very shallow dip ($< 30^\circ$). **Citation:** Bennett, R. A., S. Hreinsdóttir, M. S. Velasco, and N. P. Fay (2007), GPS constraints on vertical crustal motion in the northern Basin and Range, *Geophys. Res. Lett.*, *34*, L22319, doi:10.1029/2007GL031515.

1. Introduction

[2] The vertical component of Earth’s surface velocity field constitutes an important observable for constraining models for lithospheric loads, magmatic and hydrologic processes, and convergent and divergent tectonics. Although the Global Positioning System (GPS) is used extensively for determination of the horizontal components of the velocity field, it is rarely applied to the vertical. The precision of vertical positions determined by GPS is typically about 3–5 times lower than for the horizontal, due to a combination of unknown atmospheric propagation delays, signal multipath, and a satellite-receiving antenna geometry that precludes observations from below the horizon. This increased level of positioning noise does not by itself prohibit accurate rate estimation—to the extent that the noise in vertical position estimates is accurately represented by a combination of white and temporally correlated noise processes, vertical rate precision may be improved by increasing the number of or time span between observations [e.g., Mao *et al.*, 1999].

[3] However, determination of vertical rates also requires realization of a precise vertical datum with respect to which changes in position can be measured repeatedly. Global frames of reference for vertical surface motion are difficult to maintain using satellite-based geodesy due in large part to the continual redistribution of atmospheric, oceanic, and

continental ice and water mass, which shifts the solid Earth geocenter relative to the fluid-solid Earth center of mass about which artificial satellites orbit [Blewitt *et al.*, 2001]. Because redistribution of Earth’s fluid masses loads the crustal surface, they also cause large-scale deformations that are difficult to disentangle from geocenter translation [Tregoning and van Dam, 2005]. Another important factor limiting stability of a global vertical frame of reference is the difficulty of maintaining a consistent reference frame scale, although such sources of uncertainty have been extensively studied and largely mitigated [e.g., Schmid *et al.*, 2005]. These limitations notwithstanding, global processes and error sources should not appreciably affect relative velocities determined across regional-scale baselines. Nevertheless, surprisingly little attention has been paid to determinations of relative velocities across regional distance scales.

[4] Perhaps the best data set in the world to assess the capabilities of GPS for measurement of regional-scale vertical is in eastern Nevada and Utah (Figure 1). Permanent GPS stations in this region, which now form part of the Plate Boundary Observatory (PBO) NUCLEUS array, were originally established during the period between 1996 and 1998 for studies of regional extensional tectonics [Wernicke *et al.*, 2004] and assessment of local seismic hazards [Chang *et al.*, 2006]. The durations of the continuous time series for these stations ranges between 8.5 and 10.5 years. The formal uncertainties of secular vertical velocity estimates based on the ~ 10 -year time series of data from these stations are ≤ 0.1 mm/yr. As described above, this formal estimate of uncertainty may underestimate actual rate errors relative to an external reference frame. However, the long duration of continuous observation, density and aperture of stations, and high quality of data allows for a unique assessment of relative vertical velocity precision achievable with CGPS. Inter-site distances span the range of ~ 50 km to ~ 400 km allowing for tests of local to regional scale precision with application to numerous outstanding problems related to plate boundary zone tectonics and crustal and lithospheric loading processes.

[5] We explore the utility of long-running CGPS stations for determination of precise vertical deformation. We restrict our analyses to 12 of the longest running stations in eastern Nevada and Utah. We do not consider other long-running PBO NUCLEUS stations in central and western Nevada, the Pacific Northwest, Yellowstone, or California which have a similar history of observation, but may be affected by large-amplitude tectonic deformation [Gourmelen and Amelung, 2005; Verdonck, 2006], active mining and other anthropogenic disturbances [Gourmelen *et al.*, 2007; Bawden *et al.*, 2001], or magmatic processes [Wicks *et al.*, 2006]. We consider the effects of Great Salt

¹Department of Geosciences, University of Arizona, Tucson, Arizona, USA.

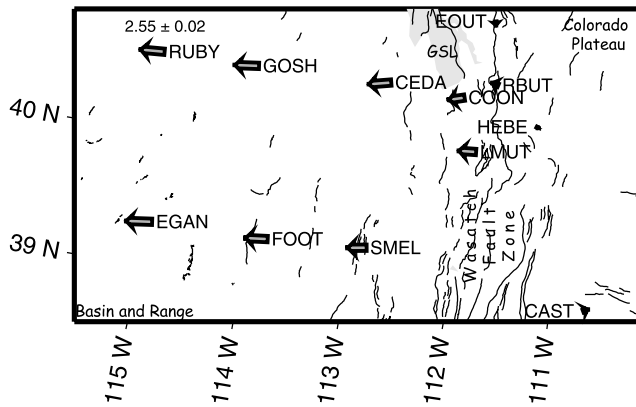


Figure 1. GPS station map with horizontal velocities relative to the Colorado Plateau. Rate uncertainties are in the range of 0.2–0.3 mm/yr. The rate of site RUBY is listed in units of mm/yr for scale. Quaternary faults are indicated by thin irregular lines. Map projection is oblique Mercator such that the horizontal axis parallels the average horizontal velocity.

Lake (GSL) loading [Elósegui *et al.*, 2003], isostatic adjustment to loss of the Laurentide ice sheet [Calais *et al.*, 2006], and strain accumulation associated with the Wasatch fault zone [Chang *et al.*, 2006].

2. GPS Data and Analysis

[6] The “test set” of GPS stations selected for our study all utilize antennas mounted on stable permanent monuments. Nine of the antennas are mounted on braced steel tripods anchored in bedrock (CAST, CEDA, COON, EGAN, FOOT, GOSH, HEBE, RUBY, SMEL). Three are mounted on single concrete encased Invar rods set in bedrock (EOUT, LMUT, RBUT). The former set of stations were constructed as part of the Basin and Range Geodetic Network (BARGEN) [Wernicke *et al.*, 2004]. The latter were constructed as part of the Eastern Basin and Range Yellowstone (EBRY) network [Chang *et al.*, 2006]. All of these stations now form part of the new PBO NUCLEUS network. We did not consider the station NAIU for this study because decadal variation in station height associated with GSL loading is expected to reach an amplitude of ≥ 3 mm [Elósegui *et al.*, 2003]. Velocity bias associated with lake loading is negligible at the other stations when averaged over the total time period, but may contribute to temporal variation in velocity estimates based on subsets of the total data set as described below.

[7] We analyzed GPS phase data using the GAMIT software package version 10.3 [King and Bock, 2005]. We processed all available data from the test set for the 10-year period, together with data from a select set of >200 regionally and globally distributed reference stations. A priori orbits and Earth orientation parameters were obtained from the International GNSS Service (IGS), but we estimated adjustments to these parameters. GPS phase data were weighted according to an elevation-angle dependent error model using an iterative analysis procedure whereby the elevation dependence was determined from the observed scatter of phase residuals. We broke the data set into ~ 50 -station subnets and resolved integer phase ambiguities

within each subnet. We applied a pole tide correction and ocean-loading model FES2004. We used IGS absolute antenna phase center models for both satellite and ground-based antennas. IGS absolute phase center models are an important new feature of high-precision GPS software packages that improves the accuracy of estimates for the vertical components of site position by mitigating reference frame scale and atmospheric mapping function errors [e.g., Schmid *et al.*, 2005].

[8] In addition to daily site position, we estimated adjustments to satellite orbital parameters, Earth orientation parameters, and time variable piecewise linear zenith and horizontal gradient tropospheric delay parameters. We used the forward Kalman filter capability of GLOBK [Herring, 2005] to estimate velocities with respect to the Stable North America Reference Frame (SNARF) Version 1.0 [Blewitt *et al.*, 2005], utilizing the full variance-covariance matrix associated with the geodetic parameter estimates for each daily GAMIT subnet solution. The frame was realized by minimizing rotation and translation parameters relative to SNARF velocities throughout the North America plate interior in order to ensure that our vertical rate estimates refer to the vertical frame implicit to SNARF. Velocity estimate uncertainties represent the formal values associated with least squares propagation of the positioning uncertainties empirically determined at the GAMIT stage as described above. We estimated phase center offsets for the BARGEN sites associated with radome changes in 1999. Parameters representing periodic signals were not estimated in determining velocities.

3. Assessment of Vertical Precision

[9] Vertical rate estimates relative to SNARF are shown in Figure 2a. Rates range between 0.0 and -1.2 mm/yr ($\sigma \leq 0.1$ mm/yr) with weighted average of -0.48 ± 0.02 mm/yr. Subsidence at the latitude of the test array is generally consistent with models for glacial isostatic adjustment (GIA) of North America, though the predictions of GIA models vary widely. For comparison, the GIA model implicit to SNARF is also shown in Figure 2a. A 0.4 ± 0.1 mm/yr systematic difference between the observed weighted-average and the average of the GIA estimates indicates systematic errors in the realization of the SNARF frame, errors in the GIA model associated with the frame, and/or real subsidence associated with other processes superimposed on the GIA signal.

[10] In order to assess the precision of relative vertical velocities among the 12 sites, we determined a local no net vertical (NNV) reference frame such that the weighted average vertical motion among test stations is zero. The advantage of the NNV frame is that any long wavelength velocity biases associated with global deformation processes and/or reference frame instability effectively cancel by differencing. The RMS vertical rate among the 12 test sites is 0.3 mm/yr. This scatter represents the combined effect of random measurement error, site-specific or short-wavelength systematic measurement error, and/or real ground motion. The rates show a clear spatial dependence; sites in the east move systematically upward relative to sites on the west. A constant velocity gradient represents the observed pattern well, with slope of 1.6 ± 0.6 nm/yr/km

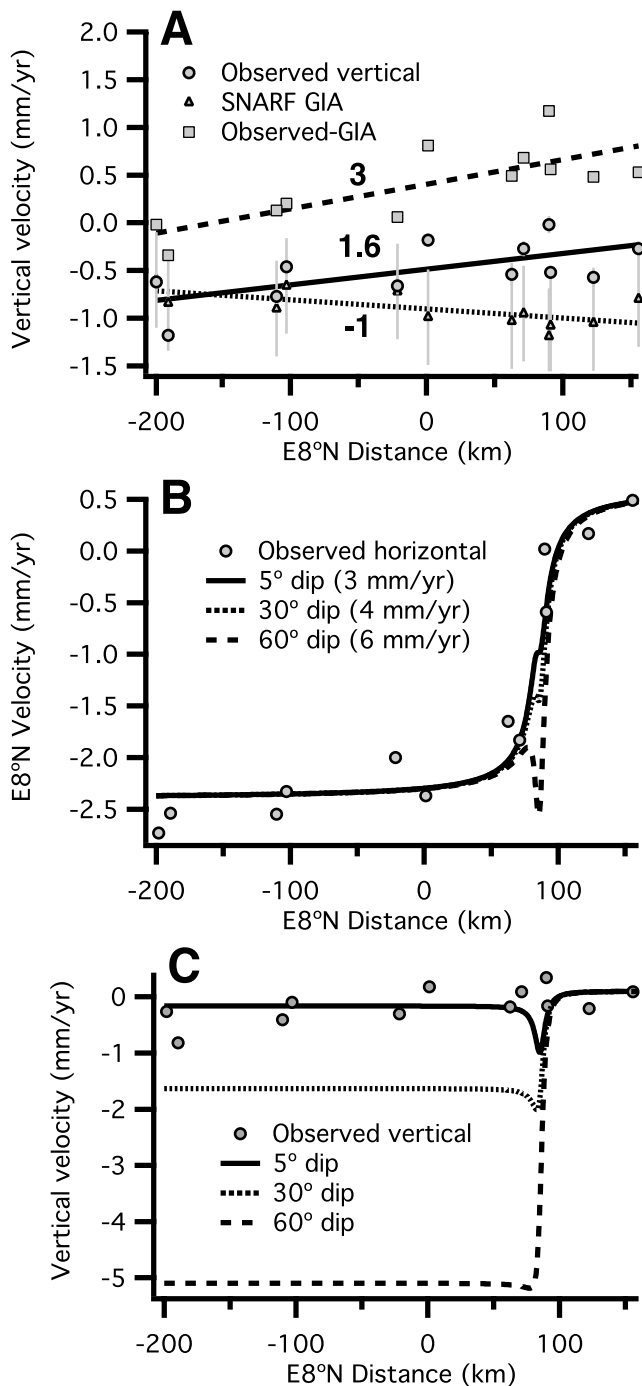


Figure 2. Velocity profiles. (a) Observed vertical rates relative to SNARF, SNARF GIA model evaluated at the GPS sites, and the observed minus SNARF rates (see text). Error bars represent $1\text{-}\sigma$ for the observed and SNARF GIA data points. Error bars are not visible for the observed rates because they are smaller than the symbols, and are not shown for the observed-minus corrected for clarity. Numbers indicate slopes of the best fit lines to each data type in units of nm/yr/km. (b) Horizontal velocities in the Colorado Plateau frame compared with three models for strain accumulation assuming dislocations in an elastic halfspace. Rates in parentheses indicate slip rates used in the respective models. (c) Same as for Figure 2b but showing vertical rates.

(Figure 2a). The observed velocities relative to SNARF can be thought of as a combined effect of GIA, tectonics, and other deformation and noise processes. Point estimates of GIA predicted by the SNARF model are uncertain at the level of ~ 0.5 mm/yr. Given these uncertainties, we calculate an insignificant gradient in vertical rates across the test network of -1.0 ± 1.3 nm/yr/km, in the opposite sense to the observed rates. Correction of the observed velocities by subtracting the GIA effect would increase the gradient of the observed velocities by a statistically insignificant amount to 2.6 ± 1.4 nm/yr/km (Figure 2a). The RMS variation of the observations corrected for GIA of 0.4 mm/yr is slightly larger than for the uncorrected rates. Given the large uncertainties associated with the GIA model, and their negligible effect on the velocity gradient across the network, we focus on the GPS observations rather than observed rates minus the SNARF GIA model.

[11] The high precision of the 10-year rates implied by the low RMS value provides a basis for an analysis of the time required to achieve vertical rate estimates of a specified precision. The duration of continuous measurement required to achieve vertical rates of a specified precision could be important, for example, for designing new experiments. Toward this end, we determined site velocities using several different continuous strands of data with varying durations starting in 2000 to avoid the effects of dome changes at BARGEN stations in 1999. Specifically, we determined velocities based on roughly seven 1-yr strands of data, six 1.5- and 2-yr strands, five 2.5- and 3-yr strands, four 3.5- and 4-yr strands, three 4.5- and 5-yr strands, two 5.5- and 6-yr strands, and one 6.5-, and 7-yr strands. Figure 3 shows the RMS differences between these rate estimates based on the partial data sets and the long term rate estimate. As expected, the difference in rate estimates decreases as the duration Δt of the data strand used to determine the estimates increases. We fit a function of the form $a\Delta t^b$ to the collection of observed RMS values, finding estimates of $\hat{a} = 2.4$ mm/yr and $\hat{b} = -1.3$. The decrease implied by these values is not as rapid as the drop in formal uncertainties based on the assumption of uncorrelated errors, which for our case decays like $2\Delta t^{-1.5}$ mm/yr (Figure 3). This small discrepancy between observed and predicted scatter likely represents some amount of temporal correlation among daily positioning errors, including possible biases associated with annual and decadal loads [Blewitt and Lavallée, 2002; Elósegui et al., 2003]. For comparison, flicker and random walk noise processes, which are commonly employed for modeling uncertainties associated with temporally correlated GPS data sets, decay like Δt^{-1} and $\Delta t^{-0.5}$, respectively, more slowly than the observed scatter of our study (Figure 3). The high precision relative to some other previous studies [e.g., Mao et al., 1999], which were based on shorter time series, may signify (1) averaging of errors over longer durations, (2) recent improvements to processing software, and/or (3) unusually favorable atmospheric or multipath observing conditions or stable monuments at the test sites.

4. Conclusions and Implications for Tectonics

[12] To illustrate the utility of combined vertical and horizontal rate estimates for tectonic applications, we show

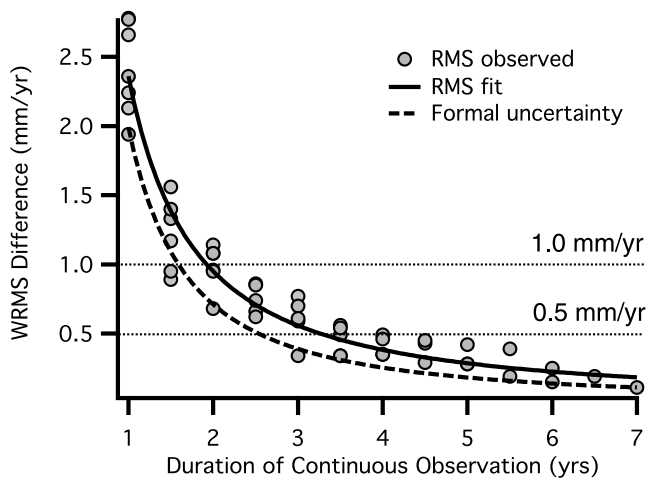


Figure 3. RMS differences between rates determined using various subsets of the total 10-year data set and the 10-yr rate. The solid curve shows a fit to the observed RMS values. The dashed curve shows the predicted standard deviation assuming white noise. The horizontal dotted lines indicate 1 mm/yr and 0.5 mm/yr for visual reference.

models for strain accumulation on the Wasatch fault zone in Figures 2b and 2c assuming deep slip on dislocations embedded in an elastic halfspace [e.g., Savage, 1983]. Three models, each with a different fault dip, are presented. Slip rates were scaled to match far field horizontal motion, such that steeper dips require faster deep slip rates (Figure 2b). For each model, the horizontal location of the dislocation edge at depth lies just west of stations EOUT and RBUT. Figure 2b shows that parameter trade-offs are such that horizontal velocities alone are relatively insensitive to the dip of the fault. In contrast, Figure 2c shows that the combination of vertical and horizontal motion is clearly sensitive to the dip of the fault. The low ~ 0.5 mm/yr net vertical displacement observed across the fault system is not consistent with models matching the horizontal rates using steeply or moderately dipping dislocations in an elastic half space; for this class of model the combined data are consistent only with very shallow dips of $\ll 30^\circ$. According to such a model, GPS measurements relate to the deeper slipping parts of the faults during the interseismic period. Slip rates inferred from such models bear indirectly on important issues related to the shallower seismogenic portions of the faults, including the mechanics of slip on low angle normal faults [e.g., Wernicke, 1995], deformation of the hanging wall [Xiao et al., 1991; Chang et al., 2006], or consistency between upper crustal slip rates inferred from paleoseismology and geomorphology with geodetically inferred rates [e.g., Friedrich et al., 2003].

[13] Malservisi et al. [2003] provide an alternative model consisting of an elastic layer overlying viscoelastic layers with lateral variations in lithospheric rheology across the Colorado Plateau–Basin and Range boundary. Models of this type are driven by constant far-field horizontal velocity boundary conditions. Extension is accommodated by pure shear such that crust and mantle lithosphere are thinned uniformly along a given vertical line [e.g., Wernicke, 1985]. Strain accumulation late in the earthquake cycle is relatively

uniformly distributed across the Basin and Range, where the model lithosphere is weak, but is lower in the Colorado Plateau region where the lithosphere is stronger. Vertical rates approach zero late in the earthquake cycle (as for the Wasatch fault zone), consistent with the observations presented above. Thus, it may be difficult to distinguish between pure and simple shear models even with precise knowledge of vertical rates late in the earthquake cycle. Another consideration is the importance of isostasy and flexure [e.g., Zandt and Owens, 1980], which could appreciably reduce the vertical component of far-field block motions relative to elastic half-space models. Additional modeling constrained by a combination of precise horizontal and vertical rate measurements is required to address these outstanding issues.

[14] **Acknowledgments.** We used data from the PBO NUCLEUS component of EarthScope. The CGPS stations used were conceived, constructed, operated, and maintained through the efforts of numerous NSF investigators and UNAVCO Facility engineers. This research benefitted from the availability of SNARF, ITRF, and IGS data products. Figure 1 was created using the GMT software. GPS data analyses were performed with the GAMIT/GLOBK analysis software. We appreciate the constructive comments of two anonymous reviewers. This study was funded by NSF EarthScope grants EAR-0441373 and EAR-0545519.

References

- Bawden, G. W., W. Thatcher, R. S. Stein, and K. W. Hudnut (2001), Tectonic contraction across Los Angeles after removal of groundwater pumping effects, *Nature*, *412*, 812–815.
- Blewitt, G., and D. Lavallée (2002), Effect of annual signals on geodetic velocity, *J. Geophys. Res.*, *107*(B7), 2145, doi:10.1029/2001JB000570.
- Blewitt, G., D. Lavallée, P. Clarke, and K. Nurutdinov (2001), A new global mode of Earth deformation: Seasonal cycle detected, *Science*, *294*, 2342–2345.
- Blewitt, G., et al. (2005), A Stable North America Reference Frame (SNARF): First release, paper presented at Annual Meeting, UNAVCO/IRIS, Stevenson, Wash., 11 June.
- Calais, E., J. Y. Han, C. DeMets, and J. M. Nocquet (2006), Deformation of the North American plate interior from a decade of continuous GPS measurements, *J. Geophys. Res.*, *111*, B06402, doi:10.1029/2005JB004253.
- Chang, W.-L., R. B. Smith, C. E. Meertens, and R. A. Harris (2006), Contemporary deformation of the Wasatch Fault, Utah, from GPS measurements with implications for interseismic fault behavior and earthquake hazard: Observations and kinematic analysis, *J. Geophys. Res.*, *111*, B11405, doi:10.1029/2006JB004326.
- Elósegui, P., J. L. Davis, J. X. Mitrovica, R. A. Bennett, and B. P. Wernicke (2003), Crustal loading near Great Salt Lake, Utah, *Geophys. Res. Lett.*, *30*(3), 1111, doi:10.1029/2002GL016579.
- Friedrich, A. M., B. P. Wernicke, N. A. Niemi, R. A. Bennett, and J. L. Davis (2003), Comparison of geodetic and geologic data from the Wasatch region, Utah, and implications for the spectral character of Earth deformation at periods of 10 to 10 million years, *J. Geophys. Res.*, *108*(B4), 2199, doi:10.1029/2001JB000682.
- Gourmelen, N., and F. Amelung (2005), Post seismic mantle relaxation in the central Nevada seismic belt, *Science*, *310*, 1473–1476.
- Gourmelen, N., F. Amelung, F. Casu, M. Manzo, and R. Lanari (2007), Mining-related ground deformation in Crescent Valley, Nevada: Implications for sparse GPS networks, *Geophys. Res. Lett.*, *34*, L09309, doi:10.1029/2007GL029427.
- Herring, T. (2005), Globk: Global Kalman filter VLBI and GPS analysis program, tech. rep., Dep. of Earth Atmos. and Planet. Sci., Mass. Inst. of Technol., Cambridge.
- King, R., and Y. Bock (2005), Documentation for the gamit GPS analysis software, tech. rep., Dep. of Earth Atmos. and Planet. Sci., Mass. Inst. of Technol., Cambridge.
- Malservisi, R., T. H. Dixon, P. C. La Femina, and K. P. Furlong (2003), Holocene slip rate of the Wasatch fault zone, Utah, from geodetic data: Earthquake cycle effects, *Geophys. Res. Lett.*, *30*(13), 1673, doi:10.1029/2003GL017408.
- Mao, A., C. G. A. Harrison, and T. H. Dixon (1999), Noise in GPS coordinate time series, *J. Geophys. Res.*, *104*, 2797–2816.
- Savage, J. (1983), A dislocation model for strain accumulation and release at a subduction zone, *J. Geophys. Res.*, *88*, 4984–4996.

- Schmid, R., M. Rothacher, D. Thaller, and P. Steingenberg (2005), Absolute phase center corrections of satellite and receiver antennas, *GPS Solutions*, *9*, 283–293.
- Tregoning, P., and T. van Dam (2005), Effects of atmospheric pressure loading and seven-parameter transformations on estimates of geocenter motion and station heights from space geodetic observations, *J. Geophys. Res.*, *110*, B03408, doi:10.1029/2004JB003334.
- Verdonck, D. (2006), Contemporary vertical crustal deformation in Cascadia, *Tectonophysics*, *417*, 221–230.
- Wernicke, B. P. (1985), Uniform-sense normal simple shear of the continental lithosphere, *Can. J. Earth Sci.*, *22*, 108–125.
- Wernicke, B. (1995), Low-angle normal faults and seismicity: A review, *J. Geophys. Res.*, *100*, 159–20,174.
- Wernicke, B., J. L. Davis, R. A. Bennett, J. E. Normandeau, A. M. Friedrich, and N. A. Niemi (2004), Tectonic implications of a dense continuous GPS velocity field at Yucca Mountain, Nevada, *J. Geophys. Res.*, *109*, B12404, doi:10.1029/2003JB002832.
- Wicks, C., W. Thatcher, D. Dzurisin, and J. Svarc (2006), Uplift, thermal unrest and magma intrusion at Yellowstone caldera, *Nature*, *440*, 72–75, doi:10.1038/nature04507.
- Xiao, H.-B., F. A. Dahlen, and J. Suppe (1991), Mechanics of extensional wedges, *J. Geophys. Res.*, *96*, 10,301–10,318.
- Zandt, G., and T. J. Owens (1980), Crustal flexure associated with normal faulting and implications for seismicity along the Wasatch front Utah, *Bull. Seismol. Soc. Am.*, *70*, 1501–1520.

R. A. Bennett, N. P. Fay, S. Hreinsdóttir, and M. S. Velasco, Department of Geosciences, University of Arizona, Tucson, AZ 85721-0077, USA. (rab@geo.arizona.edu)